

Prepared in cooperation with the U.S. Bureau of Reclamation and the Hopi Tribe

# Characterization of Subsurface Geologic Structure for Potential Water Resources near the Villages of Moenkopi, Arizona, 2009–2010

Scientific Investigations Report 2012–5180

U.S. Department of the Interior  
U.S. Geological Survey

Cover:  
Aerial photograph of the Villages of Moenkopi, Arizona. (USGS photograph taken by Jon Mason.)

# **Characterization of Subsurface Geologic Structure for Potential Water Resources near the Villages of Moenkopi, Arizona, 2009–2010**

By Jamie P. Macy

Prepared in cooperation with the U.S. Bureau of Reclamation and the Hopi Tribe

Scientific Investigations Report 2012–5180

**U.S. Department of the Interior**  
**U.S. Geological Survey**

**U.S. Department of the Interior**  
KEN SALAZAR, Secretary

**U.S. Geological Survey**  
Marcia K. McNutt, Director

U.S. Geological Survey, Reston, Virginia: 2012

For more information on the USGS—the Federal source for science about the Earth, its natural and living resources, natural hazards, and the environment, visit <http://www.usgs.gov> or call 1-888-ASK-USGS.

For an overview of USGS information products, including maps, imagery, and publications, visit <http://www.usgs.gov/pubprod>

To order this and other USGS information products, visit <http://store.usgs.gov>

Any use of trade, product, or firm names is for descriptive purposes only and does not imply endorsement by the U.S. Government.

Although this report is in the public domain, permission must be secured from the individual copyright owners to reproduce any copyrighted materials contained within this report.

Suggested citation:

Macy, J.P., 2012, Characterization of subsurface geologic structure for potential water resources near the Villages of Moenkopi, Arizona, 2009–2010: U.S. Geological Survey Scientific Investigations Report 2012–5180, 24 p. (Available at <http://pubs.usgs.gov/sir/2012/5180/>.)

# Contents

Abstract.....	1
Introduction.....	1
Purpose and Scope .....	4
Previous Investigations.....	4
Hydrogeology.....	4
Controlled Source Audio-Frequency Magnetotelluric (CSAMT) Survey .....	9
Description of Method .....	9
Collection of CSAMT Data.....	11
Characterization of Subsurface Geologic Structure .....	11
CSAMT Line A.....	11
CSAMT Line B .....	14
CSAMT Line C.....	15
CSAMT Line D.....	16
CSAMT Line E.....	17
CSAMT Line F .....	18
Conclusions.....	18
Acknowledgments .....	18
References Cited.....	18
Appendix 1. Location of Controlled Source Audio-Frequency Magnetotelluric Electrodes.....	20

# Figures

1. Map showing study area, including the Villages of Moenkopi, Arizona.....	2
2. Map showing Moenkopi supply wells and Tuba City Landfill in the study area near the Villages of Moenkopi, Arizona.....	3
3. Geologic map of the area near the Villages of Moenkopi, Arizona, 1969 .....	5
4. Geologic map of the Tuba City Landfill and adjacent Pasture Canyon near the Villages of Moenkopi, Arizona .....	6
5. Geologic map of Pasture Canyon and adjacent areas near the Villages of Moenkopi, Arizona .....	6
6. Explanation for figures 4 and 5.....	7
7. Stratigraphic columnar section for area near the Villages of Moenkopi, Arizona.....	8
8. Map showing water-table elevations near the Villages of Moenkopi, Arizona, August 2008 .....	9
9. Diagram showing controlled source audio-frequency magnetotelluric set-up .....	10
10. Graphs showing results of geophysical survey near the Villages of Moenkopi, Arizona, December, 2009 .....	12
11. Graphs showing results of geophysical survey near the Villages of Moenkopi, Arizona, December, 2009.....	13
12. Graphs showing results of geophysical survey near the Villages of Moenkopi, Arizona, April, 2010.....	14
13. Graphs showing results of geophysical survey near the Villages of Moenkopi, Arizona, April, 2010.....	15

14. Graphs showing results of geophysical survey near the Villages of Moenkopi, Arizona, April, 2010 .....	16
15. Graphs showing results of geophysical survey near the Villages of Moenkopi, Arizona, September, 2010 .....	17

## Tables

1-1. Receiver Station Location of each CSAMT electrode for Line A. ....	20
1-2. Receiver Station Location of each CSAMT electrode for Line B. ....	21
1-3. Receiver Station Location of each CSAMT electrode for Line C. ....	22
1-4. Receiver Station Location of each CSAMT electrode for Line D. ....	23
1-5. Receiver Station Location of each CSAMT electrode for Line E. ....	23
1-6. Receiver Station Location of each CSAMT electrode for Line F. ....	24

## Conversion Factors and Datums

### SI to Inch/Pound

Multiply	By	To obtain
<b>Length</b>		
meter (m)	3.281	foot (ft)
kilometer (km)	0.6214	mile (mi)
<b>Flow rate</b>		
Liter per second (Lps)	15.85	Gallons per minute (gpm)
<b>Resistivity</b>		
Ohm-meters	3.281	Ohm-foot

Vertical coordinate information is referenced to North American Vertical Datum of 1988 (NAVD 88).

Horizontal coordinate information is referenced to North American Datum of 1983 (NAD 83).

Elevation, as used in this report, refers to distance above the vertical datum.

# Characterization of Subsurface Geologic Structure for Potential Water Resources near the Villages of Moenkopi, Arizona, 2009–2010

By Jamie P. Macy

## Abstract

The Hopi Tribe depends on groundwater as their primary drinking-water source in the area of the Villages of Moenkopi, in northeastern Arizona. Growing concerns of the potential for uranium contamination at the Moenkopi water supply wells from the Tuba City Landfill prompted the need for an improved understanding of subsurface geology and groundwater near Moenkopi. Information in this report provides the Hopi Tribe with new hydrogeologic information that provides a better understanding of groundwater resources near the Villages of Moenkopi. The U.S. Geological Survey in cooperation with the U.S. Bureau of Reclamation and the Hopi Tribe used the controlled source audio-frequency magnetotelluric (CSAMT) geophysical technique to characterize the subsurface near Moenkopi from December 2009 to September 2010. A total of six CSAMT profiles were surveyed to identify possible fracturing and faulting in the subsurface that provides information about the occurrence and movement of groundwater. Inversion results from the six CSAMT lines indicated that north to south trending fractures are more prevalent than east to west. CSAMT Lines A and C showed multiple areas in the Navajo Sandstone where fractures are present. Lines B, D, E, and F did not show the same fracturing as Lines A and C.

## Introduction

Water supplies are diminishing for the Upper Village of Moenkopi and Lower Village of Moenkopi (referred to in this report as the Villages or the Villages of Moenkopi) in northeastern Arizona. The Villages are on Hopi Tribal Lands south of and topographically lower than the Navajo community of Tuba City, Arizona. (fig. 1). The Villages have a combined population of about 900–1,000 residents, and Tuba City has a population of about 8,600 (U.S. Census Bureau, 2011). Three Tribal supply wells near the Villages (fig. 2) are developed into the Navajo (N) aquifer to depths of 43, 44, and 67 meters. Navajo Tribal Utility Authority (NTUA) wells that supply Tuba City are developed much deeper in the N aquifer

and have much higher yields. The static water level and well yield in Moenkopi supply well 3 (MSW3; fig. 2) has declined substantially, by about 20 percent. Moenkopi supply well 2 (MSW2; fig. 2) has gone dry at times. The static water level in Moenkopi supply well 1 (MSW1; fig. 2), at total depth of 43 meters, has declined about 15 meters but still maintains a yield of about 2.5 liters per second. The estimated adequate water supply for the Villages is about 4.7 liters per second. Additional water resources are needed by the Hopi Tribe to address the water needs of the Villages.

Several undeveloped springs are in the Moenkopi area and at least one developed spring in the vicinity of the Villages of Moenkopi (fig. 2). The flow of the developed spring, Susunova Spring (also called Moenkopi School Spring by the U.S. Geological Survey [USGS]), has declined substantially (Macy and Brown, 2011). Flow at Susunova Spring has decreased from about 1.0 liters per second in 1987 to 0.5 liters per second in 2010. Residents of the Villages use Susunova Spring as an additional water resource.

In addition to the diminishing water supply, groundwater quality in the area of the Villages of Moenkopi may be at risk due to a possible contaminant plume of uranium and other trace elements from the Tuba City Landfill (TCL) located east of the Moenkopi supply wells (fig. 2). Maximum dissolved uranium concentrations in the plume are about 200 parts per billion, with average concentrations of about 30–40 parts per billion. The current U.S. Environmental Protection Agency (USEPA) maximum contaminant level (MCL) for public drinking-water supply is 30 parts per billion (U. S. Environmental Protection Agency, 2009). The TCL started as an unregulated waste disposal site in the 1940s. The Bureau of Indian Affairs began environmental monitoring of the TCL in 1995, and by 1997 the TCL was administratively closed due to the discovery of radionuclides in shallow groundwater at levels that exceeded the USEPA MCLs.

Growing concern about the water resources near the Villages and the possible contamination of the drinking-water source from a uranium plume near the Villages led to the involvement of the USGS to characterize subsurface geologic structure in the N aquifer near the Villages. In 2009 the U.S. Bureau of Reclamation, in cooperation with the Hopi Tribe Water Resources Program, requested the expertise of the

2 Characterization of Subsurface Geologic Structure for Potential Water Resources near the Villages of Moenkopi, Arizona

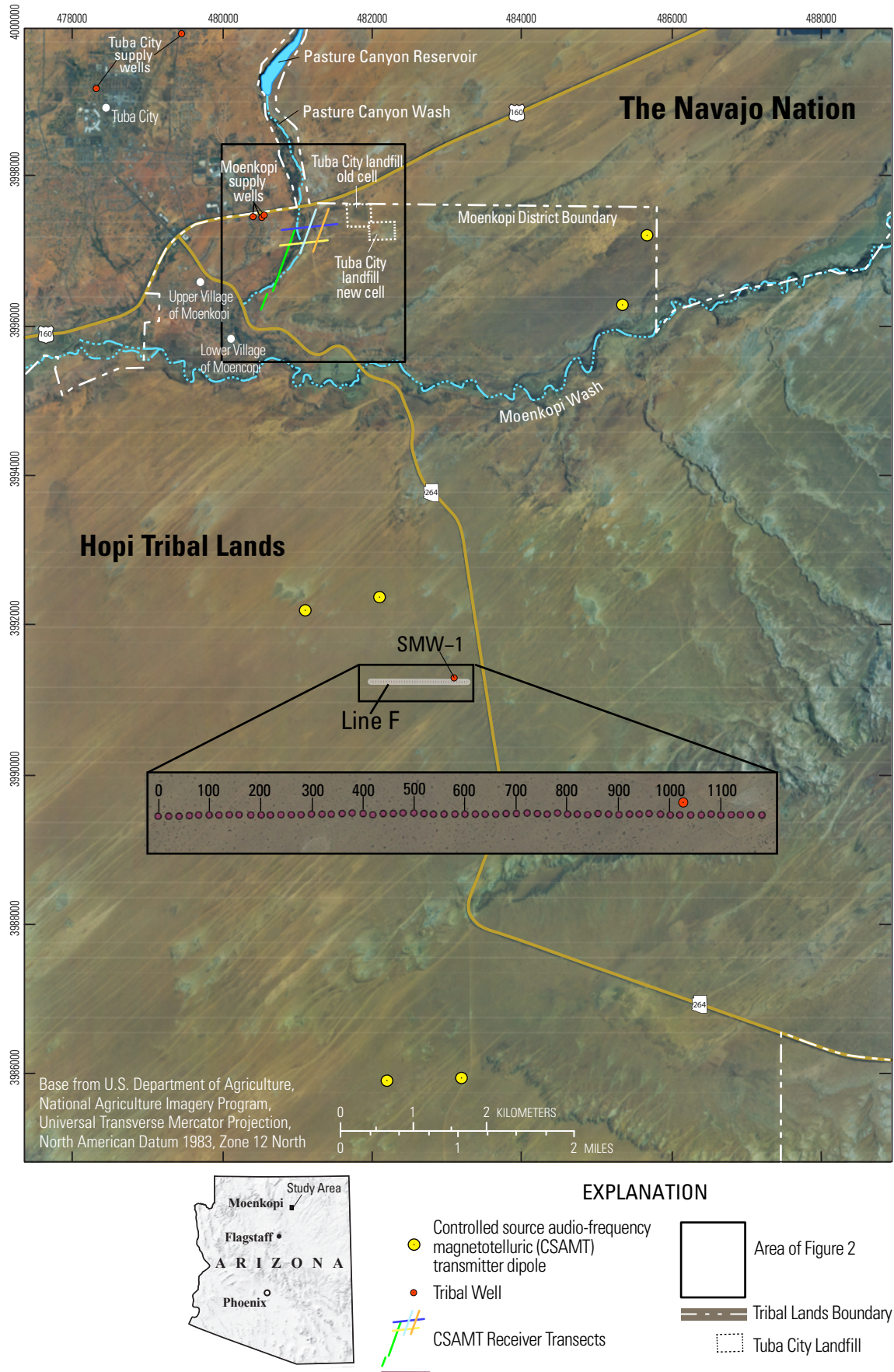
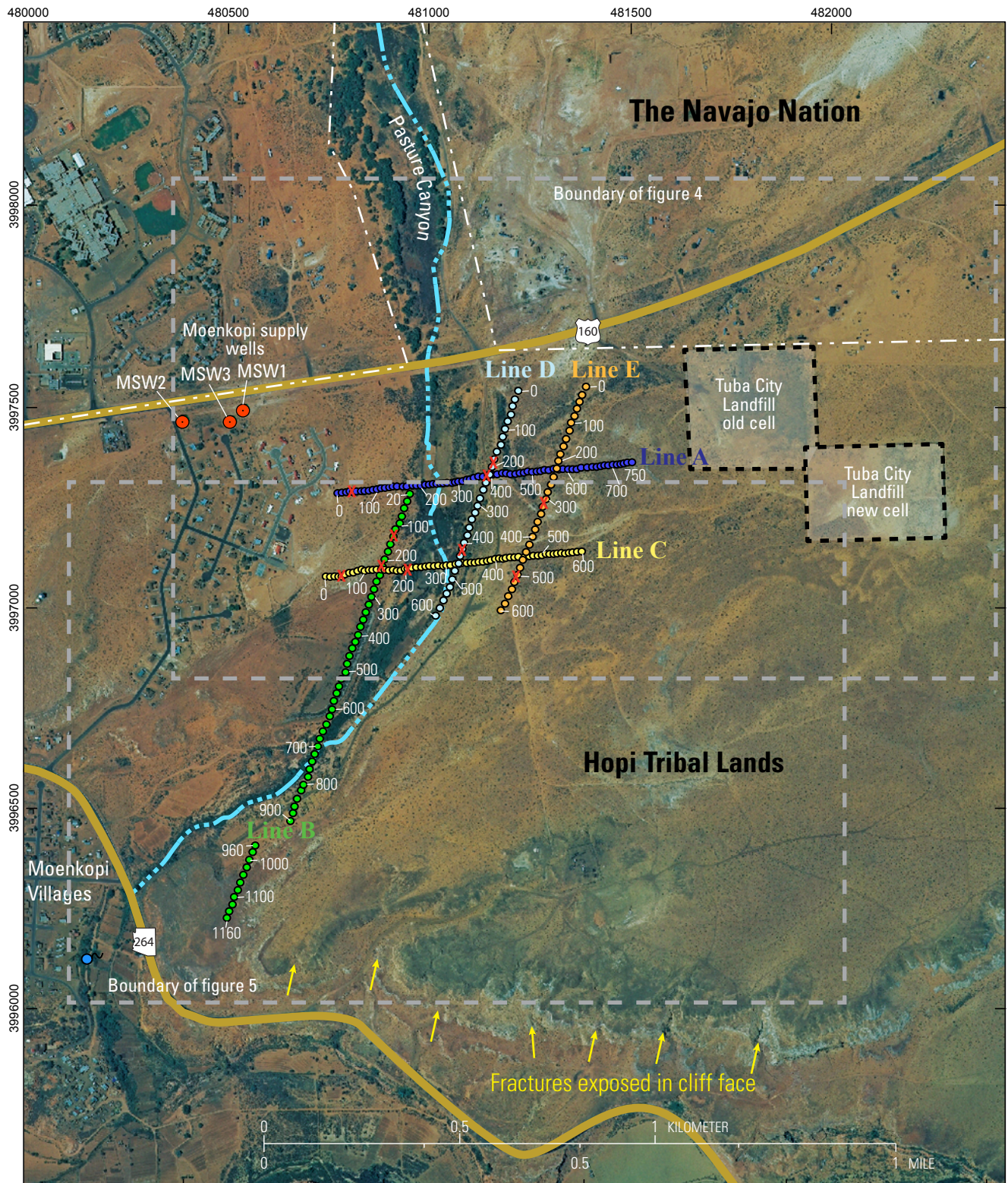


Figure 1. Map showing study area, including the Villages of Moenkopi, Arizona.



Base from U.S. Department of Agriculture, National Agriculture Imagery Program, Universal Transverse Mercator Projection, North American Datum 1983, Zone 12 North

EXPLANATION		
 Tribal well	 Tribal Lands boundary	 Area along CSAMT transect with fracture in Navajo Sandstone
 CSAMT receiver transects with electrode numbers	 Tuba City landfill site boundary	 Fractures exposed in Navajo Sandstone
 Susunova Spring	 Boundary of figures 4 & 5	

**Figure 2.** Map showing Moenkopi supply wells and Tuba City Landfill in the study area near the Villages of Moenkopi, Arizona.

## 4 Characterization of Subsurface Geologic Structure for Potential Water Resources near the Villages of Moenkopi, Arizona

USGS to better understand the occurrence and movement of groundwater near the Villages. Because the primary water-bearing zone in the area of the Villages of Moenkopi is the N aquifer, geophysical tools were used to characterize structures such as fractures within the N aquifer.

This report presents the findings from six geophysical profiles that were completed from 2009 to 2010 to define subsurface geologic structure near the Villages of Moenkopi. The geophysical technique, controlled source audio-frequency magnetotelluric (CSAMT) survey, was used as the primary tool to define subsurface structure and to provide additional information about the occurrence and movement of groundwater in the N aquifer underlying the study area. Modeled results of the CSAMT surveys are presented and discussed in relation to the local geology and groundwater-flow system.

### Purpose and Scope

The purpose of this report is to describe the findings from six geophysical surveys completed during 2009–10 near the Villages of Moenkopi. Results from these geophysical surveys will provide the Hopi Tribe with additional information about the occurrence and movement of groundwater near the Villages.

### Previous Investigations

Concerns regarding potential local contamination of drinking water from the Tuba City Landfill have led to investigations of the area near the Villages of Moenkopi. Johnson and others (2009) conducted resistivity surveys in the area of the TCL as part of an interagency agreement with the Bureau of Indian Affairs. The purpose of the study was to map the extent of the leachate plume near the TCL and better define the local groundwater system in and around the landfill. Results from the study did not indicate the presence of a conductive leachate plume, but did indicate moderately conductive zones indicative of the presence of groundwater with relatively low total dissolved solids concentrations. Northeast of the TCL, the resistivity surveys identified several shallow, conductive zones, interpreted as groundwater flow paths. Southwest of the TCL, the resistivity data indicate that groundwater flow paths converge into a single branch that flows southwesterly toward Pasture Canyon Wash.

Johnson and others (2008) presented geochemical data from the analyses of rock, sediment, and groundwater collected beneath and adjacent to the TCL. Johnson and others (2008) also performed solid-phase leaching experiments in the laboratory on solid material from the Tuba City Open Dump. In addition, a companion report (Otton and others, 2008) released geologic information and limited hydrologic and geochemical information about the TCL. Results from the study show that a section of gently northeast-dipping sedimentary rocks of Jurassic age underlies the TCL and vicinity. Surficial sediments are composed of eolian sand and fluvially reworked eolian sand that overlies the Navajo Sandstone of Jurassic age located underneath the TCL. Results

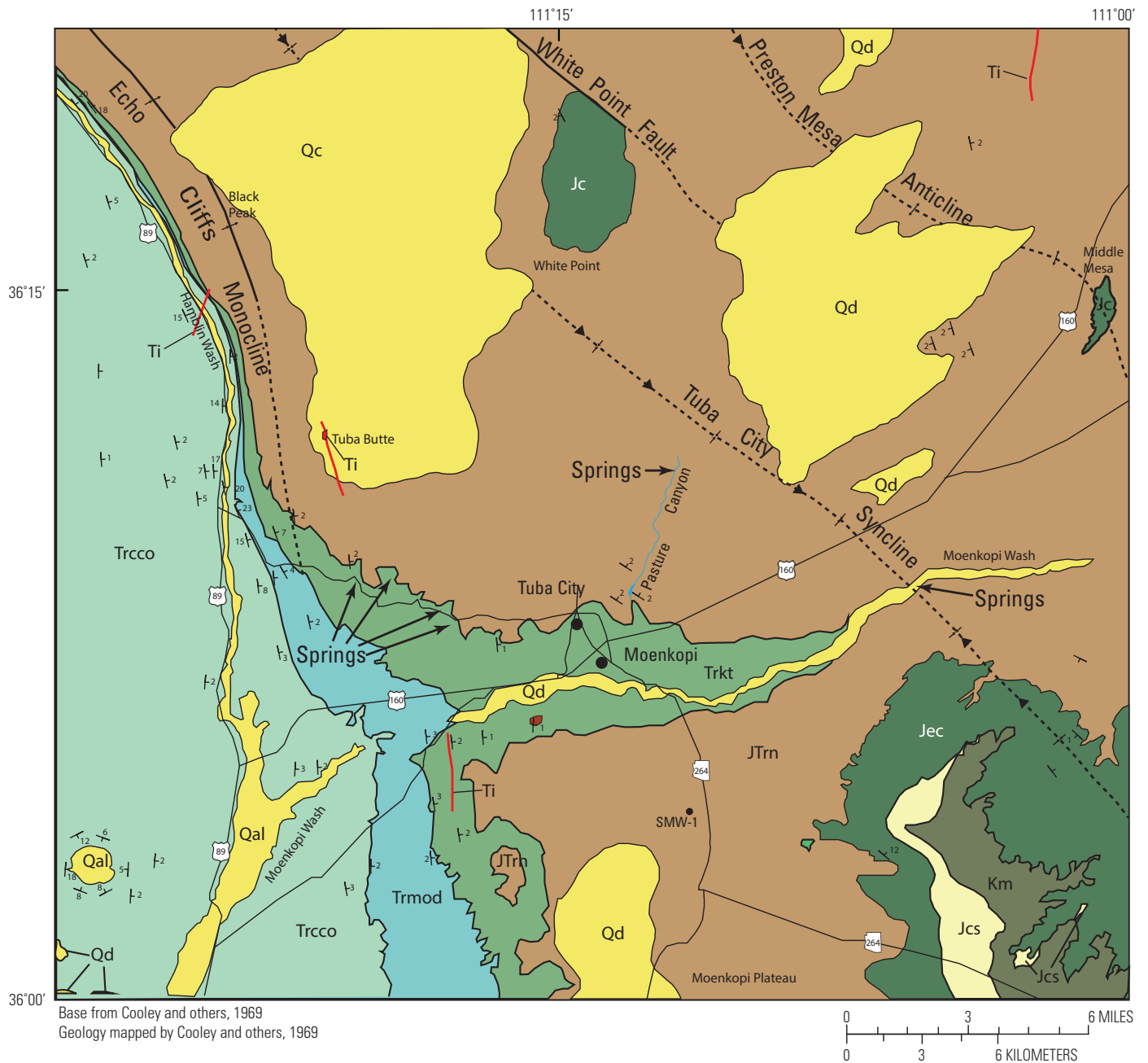
from geochemical analyses (Johnson and others, 2008) show that deeper groundwater in the Navajo Sandstone consists of dilute calcium-bicarbonate water that is low in all trace elements, including uranium. However, shallow groundwater is variably affected by near-surface processes that add varying amounts of sodium, chloride, sulfate, and trace elements, including uranium. According to Johnson and others (2008) local human influences such as the TCL could possibly affect the shallow groundwater system.

Johnson and others (2009) presents the results and interpretation of USGS data collected in and around the TCL. This report is a series of presentation slides given on March 3 and 4, 2009, in Phoenix, Ariz., for a Bureau of Indian Affairs technical meeting. The purpose of the report and presentation were to answer questions about the source of uranium and other constituents of interest in groundwater in and around the TCL. The results from the report indicate that uranium, associated major and trace elements, and other constituents of interest are stored in the vadose zone through a possible cycle of wind-blown deposition, dissolution, and concentration by evapotranspiration; thus sediments high in uranium from the Chinle Formation are blown into the area of the TCL. The sediments are deposited and come in contact with precipitation. Uranium is dissolved out of the sediments and into the water. Continual evapotranspiration concentrates the dissolved uranium. An important finding of the report was that elevated uranium and other constituents occur in shallow groundwater throughout the area, except where N aquifer water discharges at the surface as springs.

Johnson and Wirt (2009) is a follow-up report to Johnson and others (2008). The follow-up report presents the findings from geochemical data analysis of five TCL wells and of various regional rocks, sediments, groundwater, springs, and surface water. The findings focus on a comparison of the geochemistry in rocks and water in the Tuba City region. Findings from the study indicate that uranium concentrations in water near the TCL are above the concentrations typically found in the Navajo Sandstone and Kayenta Formation. In addition, this study indicates that the sources of the uranium appear to be closely related to material derived from the Chinle Formation. The Chinle Formation is exposed to the southwest of the Tuba City area and this material is potentially being transported by the dominant southwest to northeast wind direction.

### Hydrogeology

Bedrock near the Villages consists of the lower part of the Navajo Sandstone, the informally named Kayenta Formation-Navajo Sandstone transition zone (KNTZ), and the Kayenta Formation, all of Jurassic age (figs. 3-7; Cooley and others, 1969; Billingsley and others, 2007). Bedrock units in the area gently dip about 2 degrees to the northeast (Cooley and others, 1969). The Navajo Sandstone is the principal aquifer in the study area and is the primary stratigraphic unit of the N aquifer (fig. 7). The Navajo Sandstone consists of red and white, cliff-forming, crossbedded eolian sandstone and can



EXPLANATION

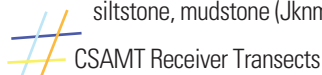
- |  |  |   |
|--|--|---|
| Qd - Dune Sand                               | Jcs - Cow Springs Sandstone (Jurassic) | Syncline, arrows along line indicated plunge direction  |
| Qal - Alluvium                               | JTrn - Navajo Sandstone (Jurassic)     | Anticline, arrows along line indicated plunge direction |
| Km - Mancos Shale                            | Trkt - Kayenta Formation (Jurassic)    | Monocline   |
| Jc - Carmel Formation                        | Trmod - Moenave Formation (Jurassic)   | Intrusive igneous rocks                                 |
| Jec - Entrada Sandstone and Carmel Formation | Trcco - Chinle Formation (Triassic)    | Strike and dip  |

Figure 3. Geologic map of the area near the Villages of Moenkopi, Arizona, 1969 (modified from Cooley and others, 1969, pl. 1).



## EXPLANATION

- Qaf** Artificial fill employed in road, reservoir, and flood-control berms. Along U.S. Highway 160 and State Highway 264, this unit also includes the asphalt pavement.
- Qg** Graded and otherwise disturbed areas that are underlain by both bedrock and sand.
- Qgb** Graded and otherwise disturbed areas underlain primarily by bedrock. May include some areas underlain by eolian sand.
- Qgs** Graded and otherwise disturbed areas underlain primarily by sand. May include some areas where weathered Navajo Sandstone is exposed. Includes one borrow pit.
- Qod** Open dump areas. Disturbed areas underlain by trash interlayered with sand used to cover the trash. Includes the old road berm that extends from the old open dump west to U.S. Highway 160. A washout in the old road berm near the Navajo-Hopi fence shows fill interlayered with domestic trash. In the new open dump area, graded areas underlain by sand with no subsurface trash are mapped with this unit. An area of bulldozed disturbed ground adjacent to the old road berm is included.
- Qps** Poned sediment. Sediment (clay, silt, and sand) deposited in low areas dammed by berms.
- Qal** Young, fine-grained sediment in the bottom of the gully that dissects the floodplain of Pasture Canyon.
- Qf** Floodplain deposits. Sediment deposited by flood waters along Pasture Canyon; this generally flat topography has been converted to agriculture in several areas (not mapped separately).
- Qt** Terrace deposits indistinguishable from Qf and mapped in Pasture Canyon below the point where a gully dissects the floodplain surface (Qf).
- Qcs** Colluvium and sheetwash deposits on gentle slopes.
- Qtc** Talus and colluvium deposits formed on steep slopes.
- Qae** Water reworked eolian or a mix of eolian and alluvial channel and floodplain deposits. This unit is mapped along the washes that pass north then west of the old open dump. It merges with the floodplain deposits along Pasture Canyon. The contact between Qf and Qae is difficult to distinguish because the area is disturbed by roads. The map unit is characterized by low topography with low vegetated hummocks. The surface of this map unit is actively being eroded by modern stream flow, and narrow incised channels as much as 1 meter deep have cut down into it southwest of the old road berm and north of U.S. Highway 160.
- Qd** Dunes and eolian sheet sand. Qdl- Dune and sheet sand areas marked by low hummocks (generally less than 1 meter high). Qdh- Hummocky dune deposits with relief to as much as 3 meters. In both areas hummocks are formed by vegetative trapping of wind-blown sediment and deflation of the intervening areas. Includes two areas of young dunes along Pasture Canyon.
- QTg** Variably cemented gravels that cap the mesa in the southeast corner of fig. 4.
- Jn** Navajo Sandstone. Jns- Sandstone, generally massively cross-bedded. Variably colored in outcrop and the subsurface. Occurs in cliff faces, on slopes below a mesa caprock. Locally forms low, ribbed outcrop areas.
- Jnl** Limestone beds within the lower Navajo Sandstone. Forms capping ledges on small mesas within the map area. Two horizons are present. One horizon caps the small mesa west and southwest of the old open dump and is probably equivalent to the limestone that caps the mesa just east of Pasture Canyon and north of U.S. Highway 160. The other horizon is a stratigraphically higher limestone that caps the mesa south of the new open dump. Exposures of the limestone in the disturbed area east of Pasture Canyon and north of U.S. Highway 160 include overlying red-brown mudstone, siltstone, and thin limestone.
- Jkn** Kayenta-Navajo transition zone sedimentary rocks. Sandstone, siltstone and mudstone undivided (Jknu), sandy siltstone, siltstone, mudstone (Jknm), sandstone (Jkns), limestone (Jknl). Mapped mostly on the west side of Pasture Canyon.



CSAMT Receiver Transects

**Figure 6.** Explanation for figures 4 and 5 (modified from Otton and others, 2008).

range in thickness from 48 to 76 m in the area of the Villages of Moenkopi (Billingsley and others, 2007). Near Tuba City, springs emerge at the contact between the Navajo Sandstone and the Kayenta Formation and are evident along Pasture Canyon, Moenkopi Wash, and the Echo Cliffs monocline (fig. 3). The Navajo Sandstone and Kayenta Formation interfinger near the Villages of Moenkopi, and the contact between these two stratigraphic units is not distinct (fig. 7). Billingsley and others (2007) informally named the rocks between the Navajo Sandstone and Kayenta Formation the KNTZ. In the study area, the KNTZ consists of alternating mudstone, siltstone, and sandstone, which likely has a local influence on shallow groundwater paths (Johnson and Wirt, 2009). The KNTZ can range in thickness from about 37 to 73 m (Billingsley and others, 2007). The Kayenta Formation underlies the Navajo Sandstone and consists of purple mudstones and siltstones interbedded with cobbles (figs. 4 and 7; Morgan, 2002). The Kayenta Formation can range in thickness from about 98 to 122 m near the Villages of Moenkopi (Billingsley and others, 2007). Although the Navajo Sandstone is the principal water-bearing unit of the N aquifer, the upper facies of the Kayenta Formation can also be water bearing (Truini and others, 2004).

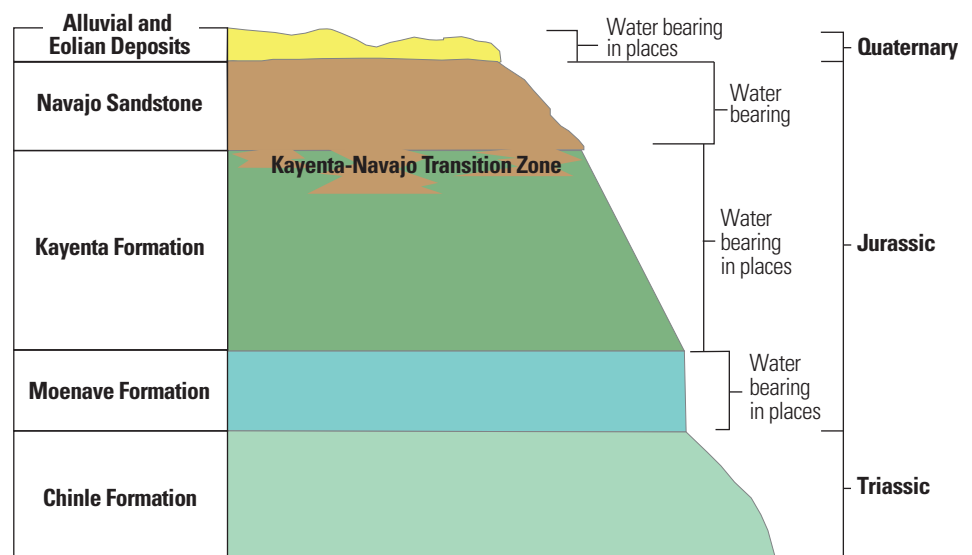
Surficial deposits near the Villages of Moenkopi consist of Quaternary eolian sand sheet and sand dune deposits, fluvial, and ponded sediments (figs. 4–6). Dune features are common and cover much of the surface near the Villages of Moenkopi (figs. 4–6). Eolian sands consist of very fine grained to fine-grained sand typically colored pale reddish-orange to moderate reddish-orange (Otton and others, 2008).

Structure in the area of the Villages of Moenkopi plays a role in the movement of groundwater. The Tuba City syncline is located about 8 kilometers to the northeast of the Villages, trends northwest to southeast, and plunges to the southeast (fig. 3). Moenkopi Wash intersects the Tuba City syncline east of the Villages. Water preferentially moves along the syncline from northwest to southeast, and springs are evident

where the syncline intersects with Moenkopi Wash. Other major geologic structures in the area also trend northwest to southeast or north-northwest to south-southeast, including the Echo Cliffs monocline. Numerous fractures have been mapped in the area of the Villages and Tuba City; fractures follow north to south, north-northwest to south-southeast, and north-northeast to south-southwest trends (George Billingsley, U.S. Geological Survey, personal commun., 2012). On the north cliff face of Moenkopi Wash to the southeast of the Villages of Moenkopi, there are numerous fractures exposed with north to south, north-northwest to south-southeast, and north-northeast to south-southwest trends (fig. 2). Fractures are often found in the areas within the Navajo Sandstone where the greatest potential for groundwater resources exist. Fractures in the Navajo Sandstone can produce large amounts of water and may provide a good source of drinking water (Truini, 1999).

The direction of groundwater movement near the TCL is west to southwest toward Pasture Canyon Wash (fig. 8). Little is known about the role Pasture Canyon Wash plays in groundwater movement, but a reservoir upstream of the study area on Pasture Canyon Wash inhibits surface water from travelling south.

Wells near the Villages of Moenkopi that were considered for this study are drilled into the Navajo Sandstone and Kayenta Formation and consist of the three Moenkopi supply wells and a single test well south of Moenkopi Wash, tribal well SMW-1 (fig. 1). Three Moenkopi supply wells are completed to depths of 43, 44, and 67 meters. Moenkopi supply well 1 (MSW1; fig. 2), land-surface elevation of 1,477 meters and total depth of 44 meters, contains sandstone, interpreted to be the Navajo Sandstone, from the land surface to a depth of about 41.5 meters. Below 41.5 meters, the sandstone layers interbed with shale and clay and represent the interfingering relation in the KNTZ. A hard, red sandy clay at 52 meters depth is interpreted as the Kayenta Formation. Moenkopi supply well 2 (MSW2; fig. 2), land-surface elevation of 1,477



Modified from Harshbarger and others (1957)

Figure 7. Stratigraphic columnar section for area near the Villages of Moenkopi, Arizona.



indication of subsurface structure (strata, faults, and fractures) and presence of groundwater (Simpson and Bahr, 2005). Grounded dipoles at the receiver site detect the electric field parallel to the transmitter, and a magnetic coil antenna senses the perpendicular magnetic field (fig. 9). The ratio of the orthogonal- and horizontal-electric field magnitudes to magnetic field magnitudes yields the apparent resistivity. CSAMT uses a remote, grounded electric dipole transmitter as an artificial signal source. The transmitter source provides a stable signal, resulting in higher precision and faster measurements than what can be obtained from natural source audio-frequency magnetotelluric (Zonge, 1992). Typically the source for a CSAMT survey should be separated from the survey line by about five times the depth of investigation because a plane wave is advantageous (fig. 9).

CSAMT measurements typically are made at frequency ranges from 1 to 8,000 hertz in binary incremental steps. For example, the frequencies of 2, 4, 8, 16, 32, 64, 128, 256, 512, 1,024, 2,048, 4,096, and 8,192 hertz would be measured. CSAMT measurements consist of orthogonal and parallel components of the electric ( $E$ ) and magnetic ( $H$ ) fields at a separation of 5 to 15 kilometers from the source (Sharma, 1997). CSAMT measurements can be taken in a number of different arrays depending on the type of information warranted. This study used a “reconnaissance” type of CSAMT array, which consists of one electric ( $E_x$ ) and one magnetic ( $H_y$ ) component for each measurement (Zonge, 1992), as opposed to a more involved survey, which collects vector and tensor measurements by measuring two electric-field components ( $E_x$  and  $E_y$ ) and three magnetic-field components ( $H_x$ ,  $H_y$ , and  $H_z$ ). Multiple electric fields are measured concurrently during reconnaissance CSAMT surveys. This study also used a six-channel receiver, which has the capability of simultaneously measuring five electric fields for every one magnetic field. Because the magnetic field does not change much over the same distance that substantial electric-field changes occur, fewer magnetic-field measurements are required. The magnetic-field measurement is used to normalize the electric fields and calculate the apparent resistivity and phase difference (Zonge, 1992). Grounded dipoles at the receiver site measure the electric field parallel to the transmitter ( $E_x$ ), and a magnetic coil antenna measures the perpendicular magnetic field ( $H_y$ ). The ratio of the  $E_x$  and  $H_y$  magnitudes

yield the apparent resistivity (equation 1; Zonge, 1992; Simpson and Bahr, 2005):

$$\rho_a = 1/5f[Ex/Hy]^2, \tag{1}$$

where  $\rho_a$  is the apparent resistivity,  $f$  is the frequency,  $E_x$  is the electrical-field strength, and  $H_y$  is the magnetic-field strength.

The penetration of CSAMT into the subsurface and the depth of investigation is determined by the skin depth (equation 2):

$$S = 503 \sqrt{(\rho_a/f)}, \tag{2}$$

where  $\rho_a$  is the measured apparent ground resistivity in ohm-meters, and  $f$  is the signal frequency (Zonge, 1992; Simpson and Bahr, 2005). The skin depth is the depth at which the amplitude of a plane wave signal has dropped to 37 percent of its value at the surface (Zonge, 1992). The skin depth is pertinent in CSAMT surveys because CSAMT data are most commonly interpreted by using simplified magnetotelluric (MT) equations, which are based on the assumption that the electric and magnetic fields behave as plane waves. Unlike MT soundings, where the source of telluric current (distant lightning strikes or atmospheric interaction with solar winds) is considered infinitely distant and nonpolarized, the CSAMT source is finite in distance and distinctly polarized (Sharma, 1997). The separation,  $r$ , between the transmitter and receiver for CSAMT surveys must be greater than three skin depths for the current driven into the ground to behave like plane waves (termed “far field”). When  $r$  is less than three skin depths at the frequency being measured, the electric and magnetic fields no longer behave as plane waves and become curved (“near field”) such that the equation for Cagniard resistivity (equation 1) no longer applies. CSAMT measurements from this study were examined for near- and far-field effects before modeling by plotting the apparent resistivity versus the frequency for a given set of soundings. All data from this study used for modeling are measured in the far field. The minimum distance between the source and receiver was 5 kilometers, yielding an  $r$  of greater than three skin depths (Zonge, 1992).

When the  $r$  between the receiver and transmitter is greater than three skin depths, the equation for depth of investigation is (Zonge, 1992):

$$D = 356 \sqrt{(\rho_a/f)}. \tag{3}$$

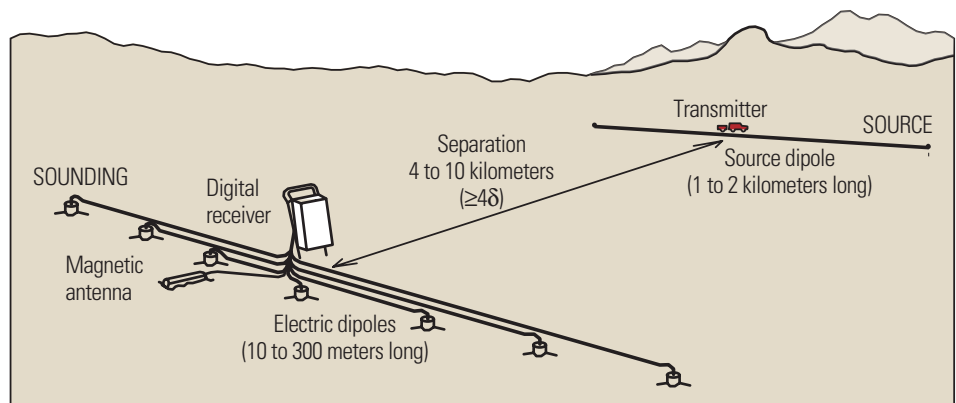


Figure 9. Diagram showing controlled source audio-frequency magnetotelluric set-up (from Zonge, 1992).

The depth ( $D$ ) of investigation of a CSAMT survey can range from 20 to 3,000 meters depending on the resistivity of the ground and the frequency of the signal. Lower frequency signals have a greater depth of investigation than higher frequency signals.

## Collection of CSAMT Data

CSAMT data were collected near the Villages of Moenkopi (fig. 2) during December 16 to 18, 2009 (Lines A and B); April 20 to 23, 2010 (Lines C, D, and E); and September 28 to 30, 2010 (Line F). A Zonge GGT-30 geophysical transmitter powered by and connected to a 25-kilowatt trailer-mounted generator, and a Zonge XMT-32 transmitter controller was used to transmit the electrical source through a 1-kilometer-long dipole. A Zonge GDP-32II multichannel geophysical receiver was connected to six porous pot electrodes arranged in 20-meter dipoles (except Line A which used a 10-meter dipole) and a Zonge ANT3 high-gain mu-metal core magnetic antenna to measure the earth's response to the transmitted signal. CSAMT field measurement set-ups consisted of one magnetic-field measurement with five accompanying electric-field measurements. Six CSAMT lines were surveyed as a part of this project, Lines A, B, C, D, E, and F (figs. 1 and 2). Three different transmitter locations were used, but each line only had one transmitter location (fig. 1). No single CSAMT line had two transmitter locations and, therefore, a single  $E_x$  and  $H_y$  field were measured at each dipole for each line. Once survey lines were complete, data were processed and analyzed using Zonge Engineering's DATPRO suite of software (Zonge Engineering, Tucson, Arizona). Raw CSAMT data were first averaged using Zonge's CSAVG program. Averaged data were reviewed for near-field and far-field effects by plotting the apparent resistivity versus the frequency (equation 2) for a given set of soundings. The lowest far-field frequency was determined, and data below that frequency, which violated the plane wave approximation because of an insufficient separation,  $r$ , were not used in the analysis. Typically for the surveys near the Villages of Moenkopi, 8 hertz was the lowest far-field frequency used for analysis. After determining the lowest far-field frequency, averaged data were entered into Zonge's SCS2D software for inversions. Data were inverted by SCS2D and examined for errors. Adjustments were made to the models in areas where the geology was known; Line F near well SMW-1 is the only place where a CSAMT survey went through well control. Final inversion models represent the best fit of collected data to model curves and are presented below.

## Characterization of Subsurface Geologic Structure

The results from inversion models of the six CSAMT surveys indicate that north-south structures are more dominant in the area of the Villages of Moenkopi than east-west structures. Modeled CSAMT data were visually displayed as a cross section for each surveyed line (figs. 10–15) and are presented and described below.

Inversion results from all lines indicate three electric layers that correlate with stratigraphic layers at depth (figs. 10B–15B). The first layer is thin and moderately conductive, 20 to 50 ohm-meters (green to yellow). This layer is interpreted as eolian sand deposits that are common in the area of the Villages of Moenkopi. The second layer is more resistive, 20 to greater than 126 ohm-meters (greater than 200 ohm-meters for Line A) and represents the Navajo Sandstone (yellow to orange to red); the unit crops out at land surface in some locations. The third layer is more conductive, about 1 to 10 ohm-meters (purple to blue) and probably represents a tongue of the Kayenta Formation within the KNTZ. In the area of the Villages of Moenkopi, the Kayenta Formation in the KNTZ can be a red-brown sandy siltstone and siltstones.

Along most lines, vertically oriented conductive areas occur within the Navajo Sandstone that probably represent large, saturated fractures. Fractures filled with water have the effect of lowering the resistivity and therefore are visible as conductive areas within a more resistive layer. These conductive areas are important because they represent possible water-filled fractures that are potentially good water resources or conduits for contaminant transport. In the area of the Villages of Moenkopi, the dominant geologic faults and fractures are in a northwest to southeast or north to south direction.

### CSAMT Line A

Line A is an east-west trending transect located parallel and just south of U.S. Highway 160 (fig. 2). Line A is 750 meters in total length, and the receiver dipole spacing is 10 meters. Inversion results from Line A indicate three stratigraphic layers with depth (fig. 10B). The first layer is thin, less than 10 meters, and moderately conductive, 20 to 50 ohm-meters (green to yellow; fig. 10). This layer is interpreted as Quaternary eolian sand deposits that are common in the area of the Villages of Moenkopi. The second layer is more resistive, 20 to greater than 200 ohm-meters, which is interpreted as the Navajo Sandstone (yellow to orange to red). The second layer is between elevations of 1,470 and 1,420 meters. In some areas, such as between electrodes 185 and 375, the resistive material is at the surface. In areas east of Pasture Canyon near electrodes 295 and 325, Navajo Sandstone is observed at the surface. The third layer of the inverse model from Line A is more conductive, about 1 to 10 ohm-meters (purple to blue) and probably represents a tongue of the Kayenta Formation within the KNTZ. This layer is below about 1,420 meters elevation. In the area of the Villages, the contact between the Navajo Sandstone and the KNTZ is a red-brown sandy siltstone and siltstones.

Two important features along Line A are the conductive areas between electrodes 35 to 65 and 385 to 415 at elevations of 1,470 to 1,420 meters. Resistivity values range from about 1 to 5 ohm-meters (purple to blue) for these features within the Navajo Sandstone layer, which typically has resistivity values of 20 to greater than 200 ohm-meters. The conductive areas within the Navajo Sandstone probably represent large

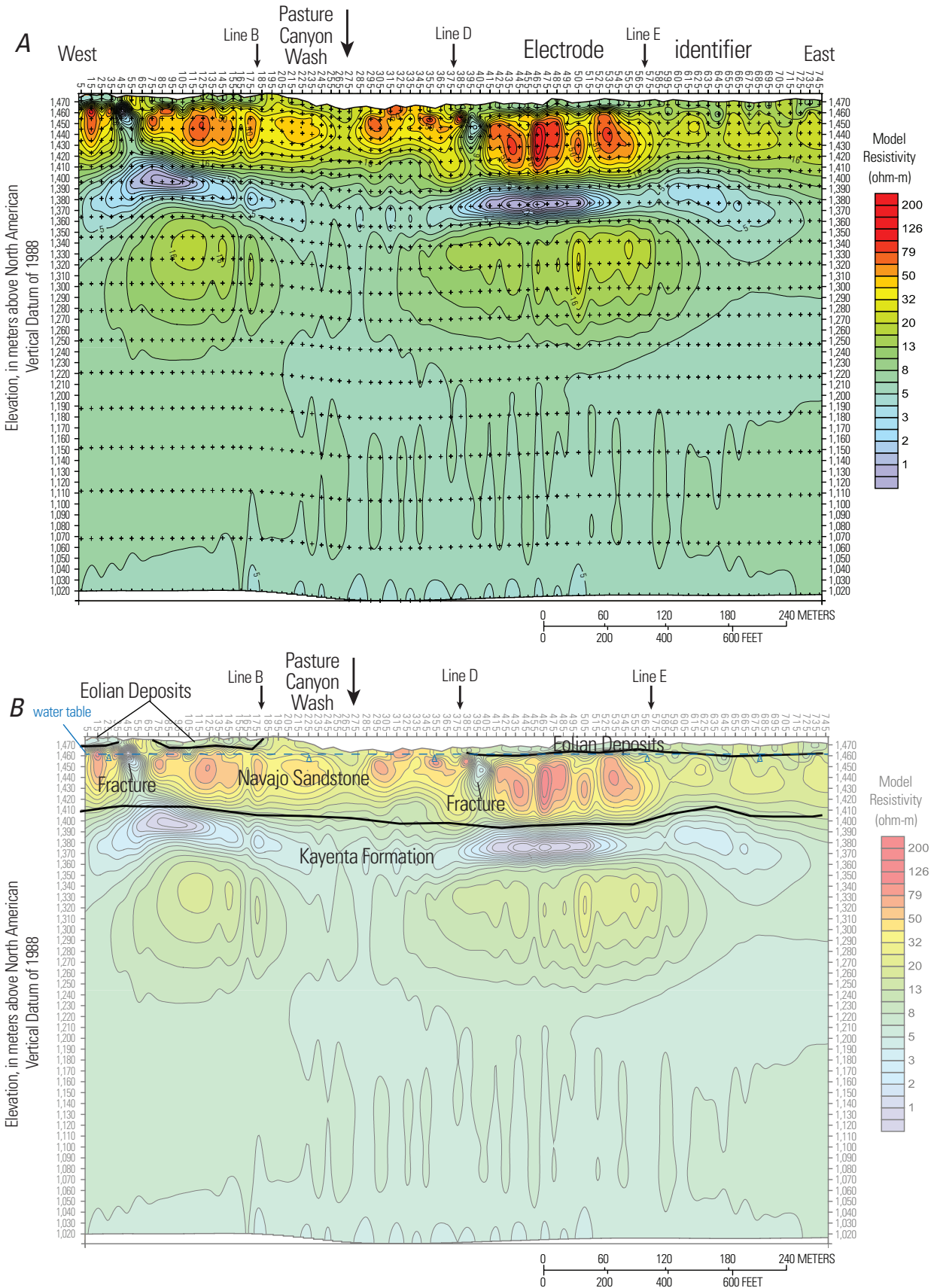


**Figure 10.** Graphs showing results of geophysical survey near the Villages of Moenkopi, Arizona, December, 2009, for Line A: *A*, West to east cross section of controlled source audio-frequency magnetotelluric, smooth-model inversion results. *B*, Interpretations of inversion results.

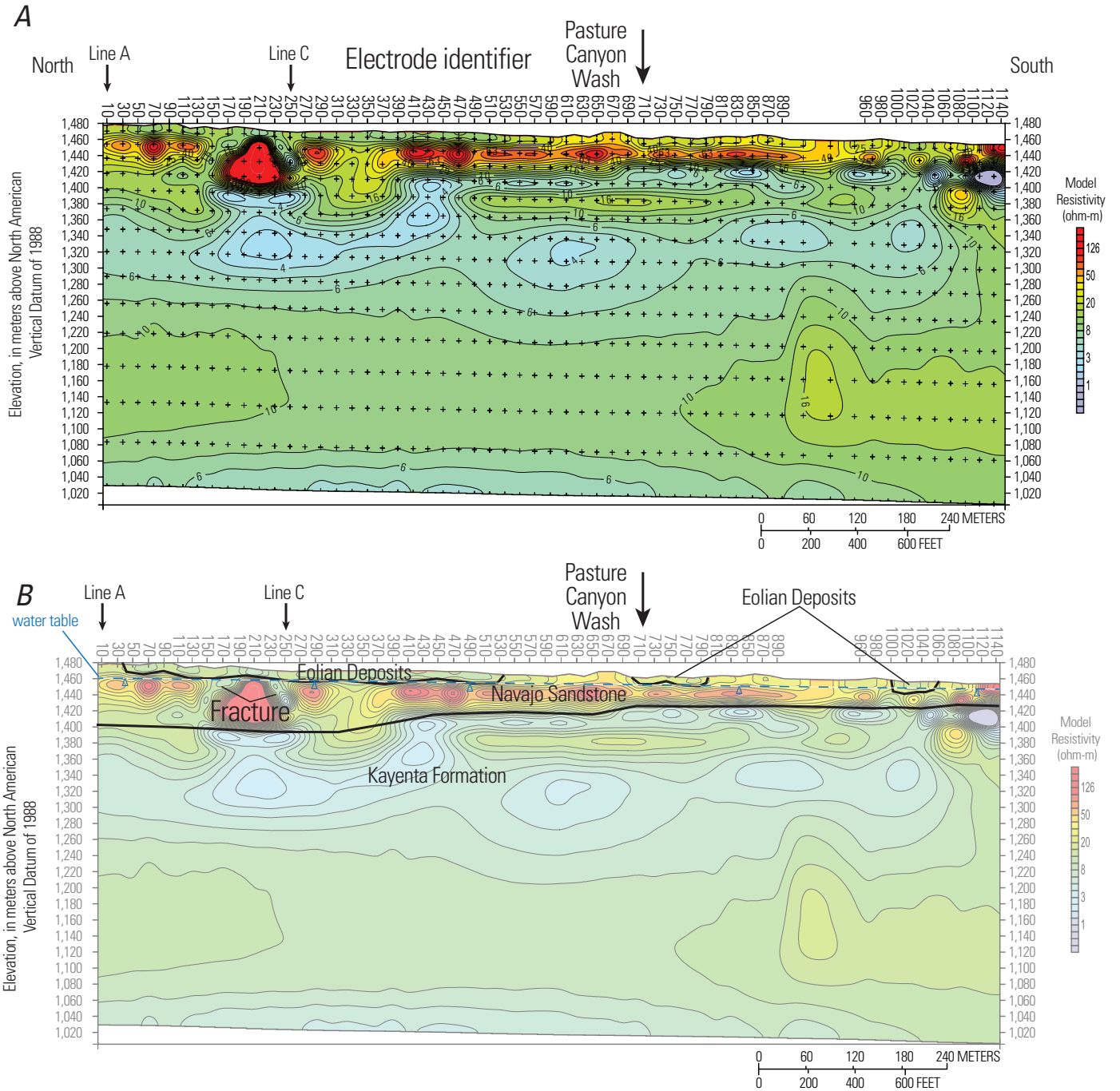


**Figure 11.** Graphs showing results of geophysical survey near the Villages of Moenkopi, Arizona, December, 2009, for Line B: **A**, North to south cross section of controlled source audio-frequency magnetotelluric, smooth-model inversion results. **B**, Interpretations of inversion results.

saturated fractures. Fractures that are filled with water have the effect of lowering the resistivity and therefore are distinguished as conductive areas within a more resistive layer. These conductive areas are important because they represent possible water-filled fractures that are potentially water bearing. In the area of the Villages Moenkopi, fractures and faults are oriented north-south.

**CSAMT Line B**

Line B is a north-south transect on the west side of Pasture Canyon Wash (fig. 2). The line originates in the area of Line A to the north and extends southward past the intersection with Pasture Canyon Wash. There is an offset to the northwest at the southern end of Line B between electrodes 900 and 960 to go around a small structure and horse corral. Inversion model results from Line B indicate three stratigraphic layers (fig. 11B). The first layer is thin, found from the surface to a depth of less than 5 meters, and moderately conductive, 20 to 50 ohm-meters (green to yellow). This layer is interpreted as eolian sand deposits that are common in the area of the Moenkopi Villages. The second layer is a more resistive area, 20 to greater than 126 ohm-meters, which is interpreted as the Navajo Sandstone (yellow to orange to red). The second layer is between elevations of 1,470 and 1,400 meters. In some areas, such as between electrodes 530 and 690, the resistive material is at the surface. The third layer of the inverse model from Line B is more conductive, about 1 to 10 ohm-meters (purple to blue), which probably represents a tongue of the Kayenta Formation within the KNTZ. This layer is below about 1,400 meters elevation.

A fracture was also crossed along Line B (fig. 11B), between electrodes 150 and 250, where conductive areas within the Navajo Sandstone layer were measured.

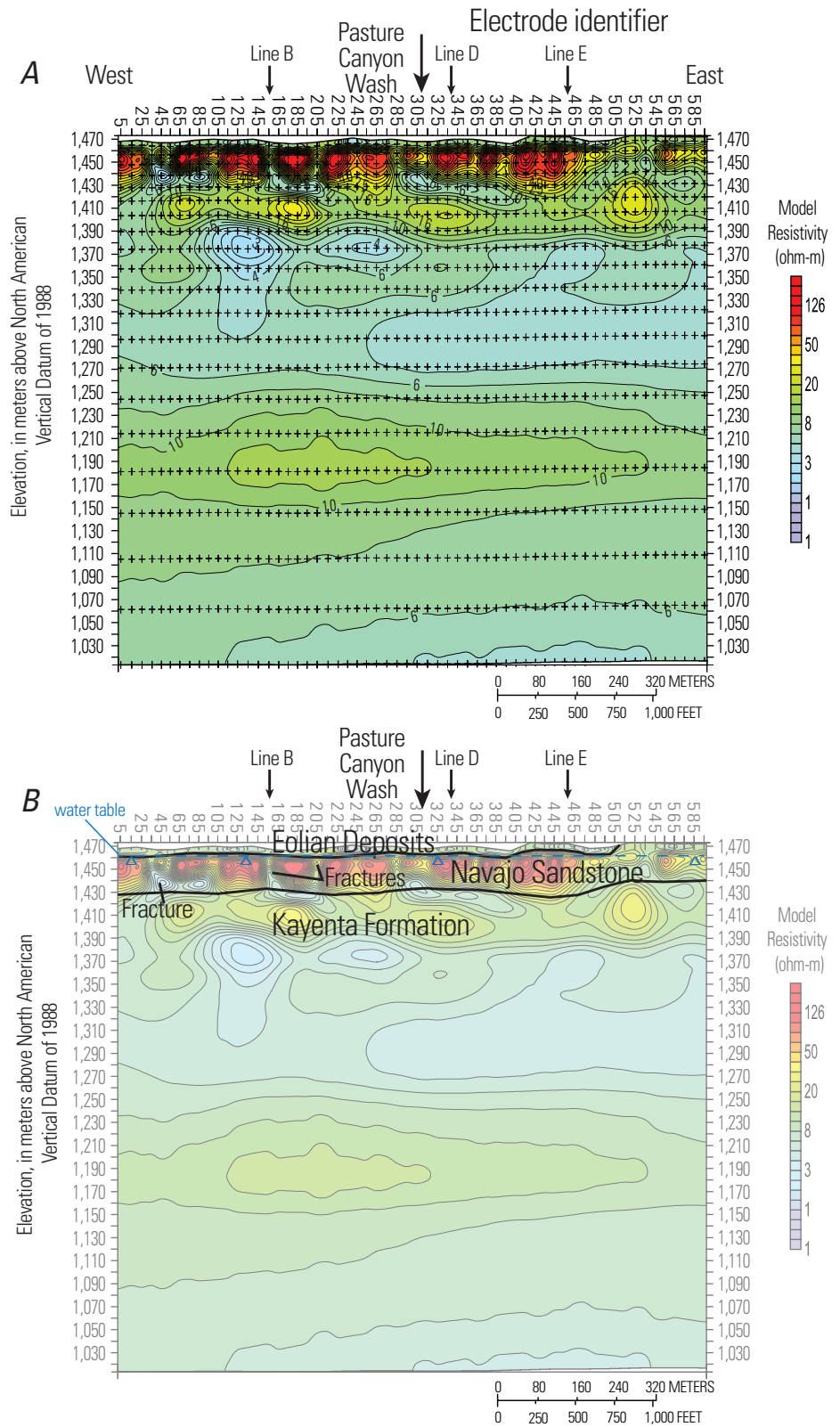


**Figure 12.** Graphs showing results of geophysical survey near the Villages of Moenkopi, Arizona, April, 2010, for Line C: A, West to east cross section of controlled source audio-frequency magnetotelluric, smooth-model inversion results. B, Interpretations of inversion results.

Most of the Navajo Sandstone layer along Line B does not show the conductive fractures except in the northernmost part of the line. Line B crosses Line C near electrode 250, and the same fracture from Line B is evident in Line C (near electrode 155; fig. 11B). Dominant structures in the area of the Villages of Moenkopi, such as the Tuba City syncline and the Echo Cliffs monocline, are northwest to southeast or north to south, and Line B could possibly be crossing a north-south fracture at an obtuse angle. So although a fracture is present on line B, it may not be indicative of east-west trending fractures.

### CSAMT Line C

Line C is an east-west transect parallel to and located about 200 meters south of Line A (fig. 2). Inversion model results from Line C indicate three stratigraphic layers (fig. 12B). The first layer is thin and moderately conductive, 20 to 50 ohm-meters (green to yellow), and present at the surface at an elevation of about 1,470 meters. This layer is interpreted as eolian sand deposits that are common in the area of Moenkopi. The second layer is more resistive, 20 to greater than 126 ohm-meters, which is interpreted as the Navajo Sandstone (yellow to orange to red). The second layer is between elevations of 1,460 and 1,430 meters. In some areas, such as between electrodes 515 and 595, the resistive material is exposed at the surface. The third layer of the inverse model from Line C is more conductive, about 1 to 10 ohm-meters (purple to blue), which probably represents a tongue of the Kayenta Formation within the KNTZ. This layer is below about 1,430 meters elevation (fig. 12).

Fractures are evident along line C. Between electrodes 35 and 55 and electrodes 155 and 205, conductive material is present within the more resistive Navajo Sandstone layer (fig. 12B). These conductive areas probably represent saturated fractures, and based on the local geology, they are oriented in a north to south manner.

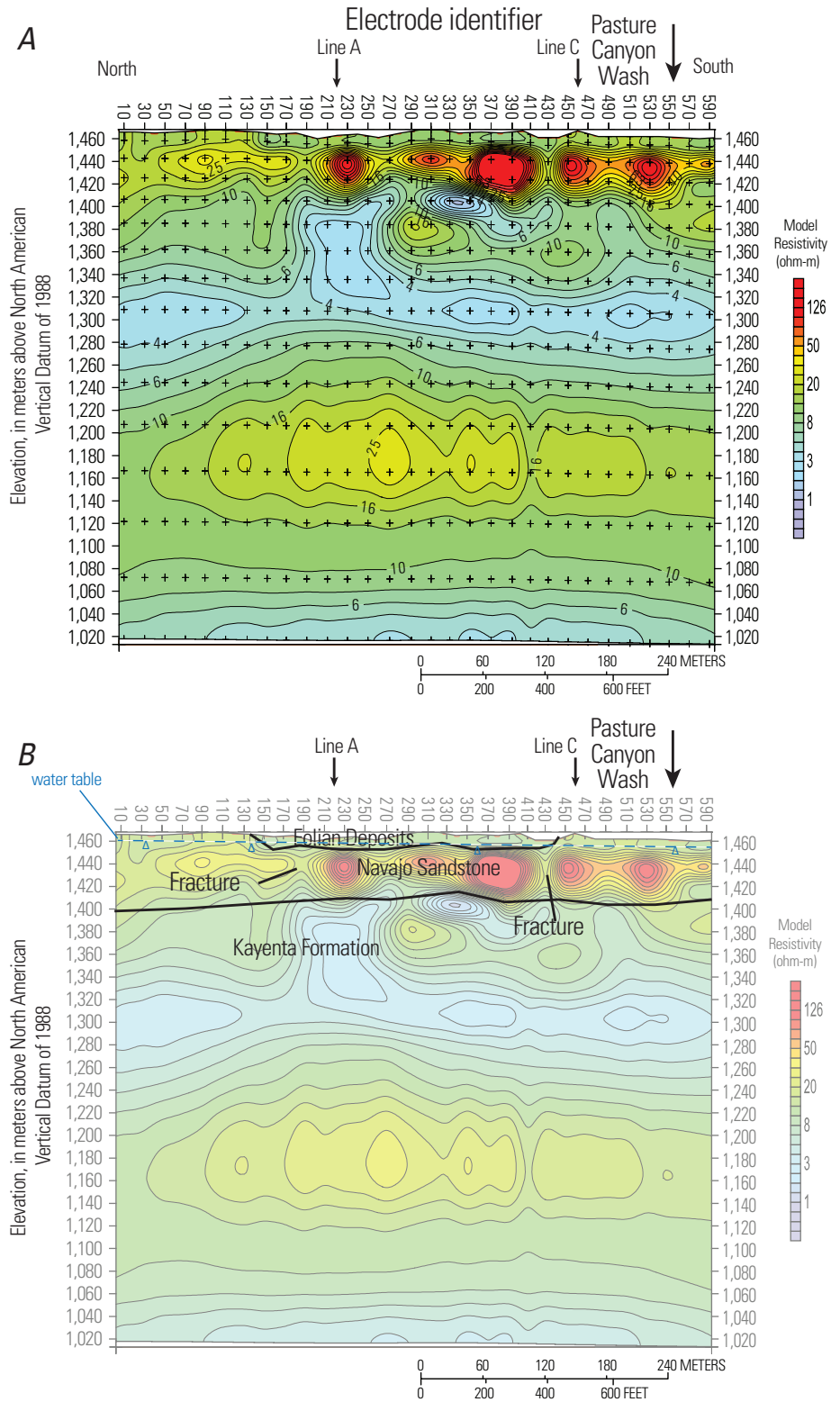


**Figure 13.** Graphs showing results of geophysical survey near the Villages of Moenkopi, Arizona, April, 2010, for Line D: A, North to south cross section of controlled source audio-frequency magnetotelluric, smooth-model inversion results. B, Interpretations of inversion results.

**CSAMT Line D**

Line D is a north to south transect parallel to Line B, but located mostly on the east side of Pasture Canyon Wash (fig. 2). Inversion model results for Line D indicate three stratigraphic layers (fig. 13B). The first layer is thin and moderately conductive, 20 to 50 ohm-meters (green to yellow), between electrodes 130 and 450. This layer is interpreted as eolian sand deposits that are common in the area of Moenkopi. The second layer is more resistive, 20 to greater than 126 ohm-meters, which is interpreted as the Navajo Sandstone (yellow to orange to red). The second layer is between elevations of 1,460 and 1,400 meters. In some areas, such as between electrodes 10 and 130 and electrodes 450 and 590, the resistive material is present

at the surface. The third layer of the inverse model from Line D is more conductive, about 1 to 10 ohm-meters (purple to blue), which probably represents a tongue of the Kayenta Formation within the KNTZ. This layer is below about 1,400 meters elevation. Below the KNTZ is the Kayenta Formation.

Near electrodes 190 and 430, resistivity values for some areas are as low as 10 to 20 ohm-meters. Although those areas could potentially be fractures, they do not look the same as other fracture areas in the Navajo Sandstone (not as conductive as fractures on Line A [1 to 5 ohm-meters; fig. 10B] or on Line C [1 to 10 ohm-meters; fig. 12B]). Whether or not those areas are fractures cannot be definitively determined, but based on other evidence in the area, they do not appear to be saturated fractures.

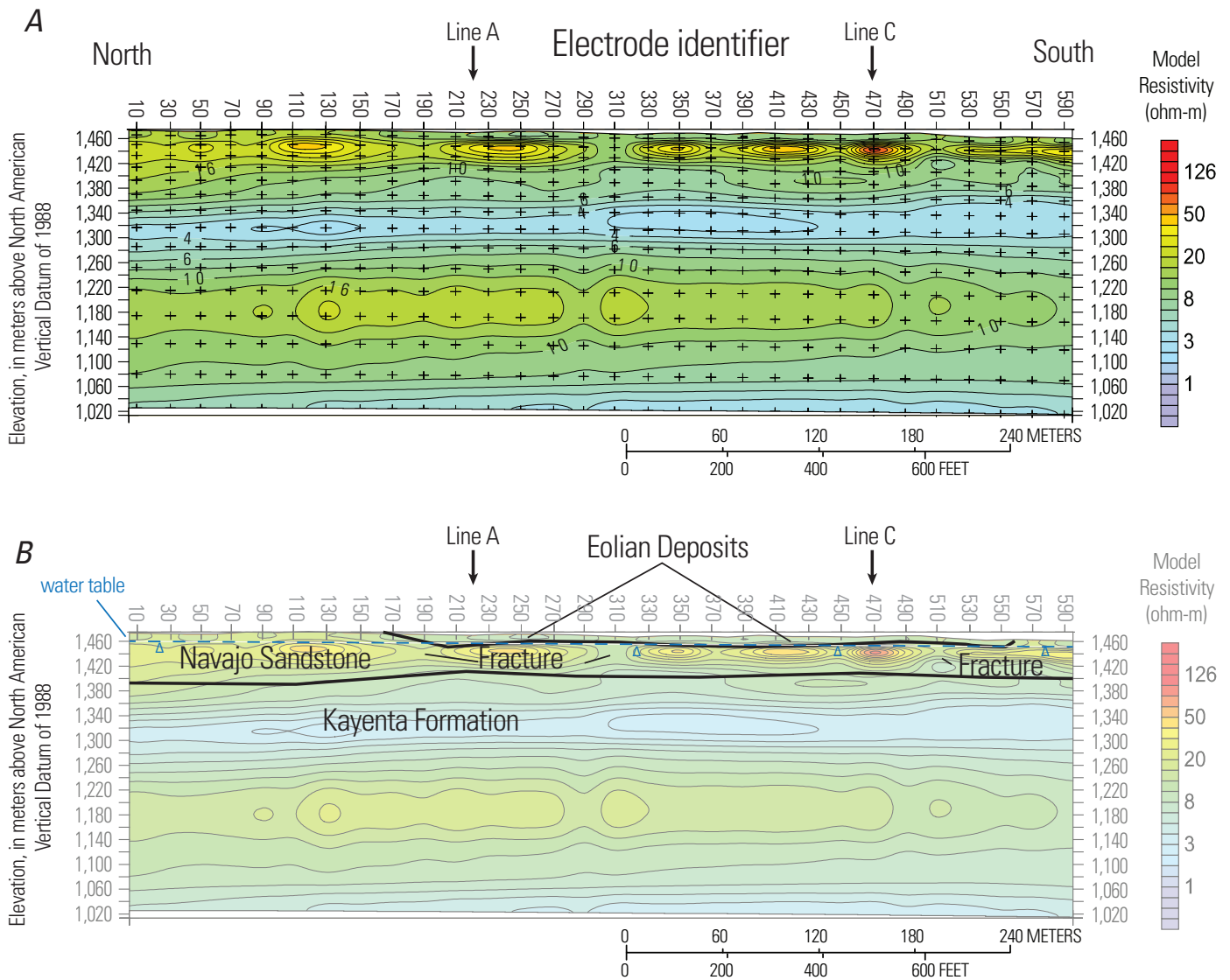


**Figure 14.** Graphs showing results of geophysical survey near the Villages of Moenkopi, Arizona, April, 2010, for Line E: *A*, North to south cross section of controlled source audio-frequency magnetotelluric, smooth-model inversion results. *B*, Interpretations of inversion results.

### CSAMT Line E

Line E is a north to south transect parallel to Lines B and D and located east of Pasture Canyon Wash (fig. 2). Inversion results from Line E indicate three stratigraphic layers (fig. 14B). The first layer is thin and moderately conductive, 20 to 50 ohm-meters (green to yellow) between electrodes 170 and 550. This layer is interpreted as eolian sand deposits

that are common in the area of Moenkopi. The second layer is more resistive, 20 to greater than 126 ohm-meters, which is interpreted as the Navajo Sandstone (yellow to orange to red). The second layer is between elevations of 1,460 and 1,400 meters. In some areas, such as between electrodes 10 and 150 and electrodes 550 and 590, the resistive material is present at the surface. The third layer of the inverse model from Line E is more conductive, about 1 to 10 ohm-meters (purple to blue),

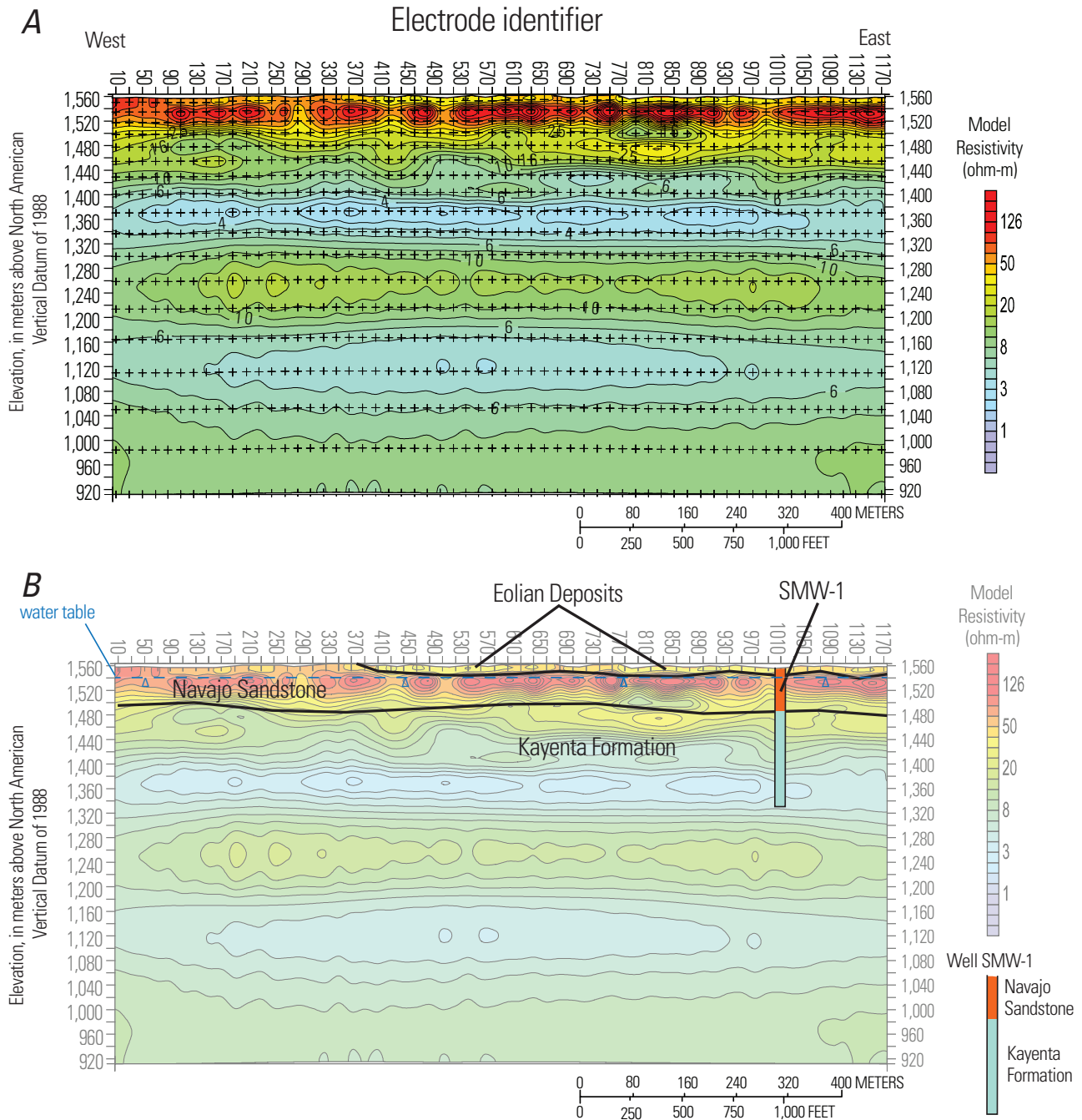


**Figure 15.** Graphs showing results of geophysical survey near the Villages of Moenkopi, Arizona, September, 2010, for Line F: *A*, West to east cross section of controlled source audio-frequency magnetotelluric, smooth-model inversion results. *B*, Interpretations of inversion results.

which probably represents a tongue of the Kayenta Formation within the KNTZ. This layer is below about 1,400 meters elevation. Below the KNTZ is the Kayenta Formation.

One potential fracture area along Line E is near electrode 310 (fig. 14*B*). The resistivity values are between 8 and 20 ohm-meters from the land surface to an elevation of about 1,400 m. The fracture appears as a vertical conductive feature between a semi-continuous high resistivity unit. Although other fractures in the Navajo Sandstone layer are typically closer to 1 to 10 ohm-meters, this area is potentially a fracture.

## CSAMT Line F

Line F is an east to west transect located about 4 kilometers south of Moenkopi Wash (fig. 1). Line F was surveyed for potential water resources south of Moenkopi Wash in the area where there is an existing N aquifer well, SMW-1. Inversion model results from Line F indicate three stratigraphic layers (fig. 15*B*). The first layer is thin and moderately conductive, 20 to 50 ohm-meters (green to yellow), between electrodes 370 and 1,190. This layer represents eolian sand deposits that are common in the area near the Villages of Moenkopi. The second layer is more resistive, 20 to greater than 126 ohm-meters, which is interpreted as the Navajo Sandstone (yellow to orange to red). The second layer is between elevations of 1,550 and 1,480 meters. In some areas, such as between electrodes 10 and 370, the resistive material is present at the surface. The third layer is more conductive, about 1 to 10 ohm-meters (purple to blue), which probably represents a tongue of the Kayenta Formation within the KNTZ. This layer is below about 1,480 meters elevation. Below the KNTZ is the Kayenta Formation. An N aquifer test well, SMW-1 (fig. 1), was drilled in the area of Line F near electrode 1,030, and the driller's log describing Navajo Sandstone and Kayenta Formation resembles the geophysical survey (fig. 15*B*).

## Conclusions

Data from this study indicate that fractures are present in the Navajo Sandstone, primarily in a north to south orientation. Fractures identified along Line A and Line C could hold potential water resources. Large fractures were not identified along Line F. North to south survey Lines B, D, and E do not show large fracturing, but they do show some fractures. While the lack of large fractures in an east to west orientation suggests minimal potential for developing additional water resources, it does however suggest that the movement of contaminated water to the Moenkopi supply wells would be inhibited. The movement of groundwater near Moenkopi can be northeast to southwest or east to west and the presence of east to west fractures in the Navajo Sandstone could work to more easily move contaminated material through the subsurface towards the Moenkopi Supply Wells. Inversion results from geophysical surveys indicate that east to west fractures are present, but they are not as large as north to south fractures.

## Acknowledgments

The author would like to thank the Hopi Tribe for their support of the project, access to Tribal lands for research, and insight into water resources near the Villages of Moenkopi. The author would also like to extend his appreciation to the Upper Village of Moenkopi and the Lower Village of Moenkopi for their cooperation during the project. Appreciation is also extended to the Hopi Water Resources Department, and to Lionel Puhuyesva, Director of the Hopi Water Resources Department. The field staff from the U.S. Geological Survey Arizona Water Science Center is owed a debt of gratitude for their hard work in often perilous field conditions; specifically the author would like to thank Geoff DeBenedetto, Chris Brown, Corey Sannes, Curt Crouch, and Kurt Schonauer.

## References Cited

- Billingsley, G.H., Priest, S.S., and Felger, T.L., 2007, Geologic map of the Cameron 30' x 60' quadrangle, Coconino County, northern Arizona: U.S. Geological Survey Scientific Investigations Map 2977, scale 1:100,000, 33 p.
- Cooley, M.E., Harshbarger, J.W., Akers, J.P., and Hardt, W.F., 1969, Regional hydrogeology of the Navajo and Hopi Indian reservations, Arizona, New Mexico, and Utah: U.S. Geological Survey Professional Paper 521-A, 61 p.
- Harshbarger, J.W., Repenning, C.A., and Irwin, J.H., 1957, Stratigraphy of the Uppermost Triassic and the Jurassic Rocks of the Navajo Country: U.S. Geological Survey Professional Paper 291, 71 p.
- Johnson, R.H., and Wirt, Laurie, 2009, Geochemical analyses of rock, sediment, and water from the region in and around the Tuba City Landfill, Tuba City, Arizona: U.S. Geological Survey Open-File Report 2009-1020, 44 p.
- Johnson, R.H., Otton, J.K., Horton, R.J., Gallegos, T.J., Choate, L.M., and Sullivan, J.E., 2008, Geochemical data from analyses of rock, sediment, water, and solid-phase leaching at the Tuba City Open Dump, Tuba City, Arizona: U.S. Geological Survey Open-File Report 2008-1374, 10 p.
- Johnson, R. H., Otton, J.K., and Horton, R.J., 2009, Results and interpretations of U.S. Geological Survey data collected in and around the Tuba City Open Dump, Arizona: U.S. Geological Survey Open-File Report 2009-1154, 125 p.
- Macy, J.P., and Brown, C.R., 2011, Groundwater, surface-water, and water-chemistry data, Black Mesa area, northeastern Arizona—2009-10: U.S. Geological Survey Open File Report 2011-1198, 42 p.

- Morgan, R., 2002, Rapid site characterization report—The Hopi Tribe Water Resources Program: Prepared under the U.S. Environmental Protection Agency Resource and Conservation and Recovery Act Section 8001 Grant Project, 110 p.
- Otton, J.K., Johnson, R.H., and Horton, R.J., 2008, Geologic maps and cross sections of the Tuba City open dump site and vicinity, with implication for the occurrence and flow of groundwater: U.S. Geological Survey Open-File Report 2008–1380, 78 p.
- Sharma, P.V., 1997, Environmental and engineering geophysics: Cambridge, Cambridge University Press, XXX p.
- Simpson, Fiona, and Bahr, Karsten, 2005, Practical magnetotellurics: Cambridge, Cambridge University Press, 254 p.
- Truini, Margot, 1999, Geohydrology of Pipe Spring National Monument Area, Northern Arizona: U.S. Geological Survey Water-Resources Investigations Report 98–4263, 25 p.
- Truini, Margot, Fleming J.B., and Pierce, H.A., 2004, Preliminary Investigation of structural controls of groundwater movement in Pipe Spring National Monument, Arizona: U.S. Geological Survey Scientific Investigations Report 2004–5082, 16 p.
- Zonge, K.L., 1992, Broad band electromagnetic systems, *in* Van Blaricom, Richard, ed., Practical geophysics II for the exploration geologist: Northwest Mining Association, p. 439–523.
- Zonge Engineering, Software, 2006, CSINV Documentation: Tucson, Arizona, Zonge Engineering Inc., 29 p.

## Appendix 1. Location of Controlled Source Audio-Frequency Magnetotelluric Electrodes

**Table 1-1.** Receiver Station Location of each CSAMT electrode for Line A.

[Coordinate system: Universal Transverse Mercator Zone 11, North American Datum of 1983; elevation is in meters above the North American Vertical Datum of 1988]

Electrode identifier	Northing (meters)	Easting (meters)	Elevation (meters)	Electrode identifier	Northing (meters)	Easting (meters)	Elevation (meters)
0	480724	3997488	1473	380	481100	3997529	1467
10	480732	3997491	1477	390	481109	3997531	1468
20	480743	3997491	1476	400	481118	3997535	1467
30	480752	3997494	1478	410	481128	3997537	1468
40	480764	3997492	1474	420	481138	3997540	1470
50	480773	3997493	1476	430	481146	3997538	1468
60	480783	3997497	1475	440	481157	3997537	1469
70	480793	3997496	1475	450	481167	3997538	1468
80	480803	3997497	1474	460	481175	3997539	1469
90	480813	3997498	1474	470	481185	3997540	1467
100	480823	3997500	1472	480	481194	3997541	1473
110	480833	3997502	1474	490	481204	3997544	1472
120	480843	3997503	1475	500	481214	3997543	1469
130	480853	3997504	1478	510	481227	3997545	1470
140	480862	3997505	1475	520	481237	3997547	1471
150	480873	3997507	1477	530	481247	3997548	1473
160	480883	3997507	1477	540	481256	3997547	1472
170	480889	3997505	1474	550	481265	3997549	1471
180	480902	3997507	1476	560	481276	3997549	1470
190	480912	3997508	1478	570	481286	3997548	1471
200	480922	3997509	1477	580	481297	3997548	1472
210	480933	3997508	1474	590	481305	3997548	1470
220	480942	3997510	1473	600	481316	3997548	1472
230	480953	3997510	1470	610	481326	3997548	1471
240	480961	3997512	1466	620	481335	3997551	1470
250	480973	3997512	1468	630	481345	3997552	1471
260	480980	3997513	1465	640	481355	3997553	1470
270	480989	3997513	1463	650	481366	3997554	1470
280	480999	3997515	1465	660	481375	3997556	1471
290	481011	3997516	1466	670	481386	3997557	1470
300	481020	3997517	1464	680	481395	3997559	1469
310	481029	3997520	1463	690	481405	3997559	1470
320	481040	3997521	1467	700	481415	3997561	1470
330	481050	3997524	1465	710	481427	3997561	1472
340	481060	3997526	1467	720	481437	3997562	1473
350	481068	3997527	1466	730	481447	3997563	1472
360	481078	3997532	1464	740	481455	3997565	1472
370	481089	3997530	1468	750	481465	3997565	1471

**Table 1-2.** Receiver Station Location of each CSAMT electrode for Line B.

[Coordinate system: Universal Transverse Mercator Zone 11, North American Datum of 1983; elevation is in meters above the North American Vertical Datum of 1988]

Electrode identifier	Northing (meters)	Easting (meters)	Elevation (meters)	Electrode identifier	Northing (meters)	Easting (meters)	Elevation (meters)
0	480910	3997507	1477	560	480718	3996989	1465
20	480905	3997488	1479	580	480712	3996970	1464
40	480897	3997469	1478	600	480707	3996951	1463
60	480890	3997451	1477	620	480701	3996930	1466
80	480882	3997431	1480	640	480695	3996912	1463
100	480877	3997414	1480	660	480685	3996895	1469
120	480869	3997398	1474	680	480677	3996877	1469
140	480863	3997379	1476	700	480671	3996858	1462
160	480855	3997362	1473	720	480663	3996838	1461
180	480848	3997341	1476	740	480658	3996820	1464
200	480842	3997323	1474	760	480650	3996801	1462
220	480835	3997305	1471	780	480646	3996781	1461
240	480828	3997286	1470	800	480637	3996763	1463
260	480821	3997268	1469	820	480629	3996747	1464
280	480813	3997249	1470	840	480620	3996727	1463
300	480807	3997229	1470	860	480613	3996707	1466
320	480800	3997211	1470	880	480608	3996690	1464
340	480793	3997192	1470	900	480603	3996671	1460
360	480786	3997174	1471	950	480514	3996611	1458
380	480780	3997155	1469	970	480508	3996593	1460
400	480773	3997136	1470	990	480500	3996574	1462
420	480766	3997118	1470	1010	480492	3996554	1455
440	480759	3997101	1470	1030	480485	3996537	1457
460	480753	3997082	1469	1050	480476	3996519	1456
480	480745	3997062	1469	1070	480470	3996499	1457
500	480741	3997042	1468	1090	480462	3996482	1454
520	480731	3997026	1466	1110	480458	3996464	1453
540	480725	3997008	1465	1130	480449	3996447	1455
				1150	480443	3996430	1453

## 22 Characterization of Subsurface Geologic Structure for Potential Water Resources near the Villages of Moenkopi, Arizona

**Table 1-3.** Receiver Station Location of each CSAMT electrode for Line C.

[Coordinate system: Universal Transverse Mercator Zone 11, North American Datum of 1983; elevation is in meters above the North American Vertical Datum of 1988]

Electrode identifier	Northing (meters)	Easting (meters)	Elevation (meters)	Electrode identifier	Northing (meters)	Easting (meters)	Elevation (meters)
0	480752	3997083	1472	330	481077	3997117	1463
10	480763	3997085	1469	340	481087	3997118	1462
20	480773	3997086	1468	350	481096	3997120	1463
30	480783	3997084	1471	360	481108	3997120	1463
40	480791	3997084	1475	370	481119	3997120	1463
50	480802	3997092	1469	380	481128	3997119	1465
60	480811	3997095	1473	390	481137	3997121	1466
70	480822	3997096	1473	400	481147	3997122	1463
80	480832	3997099	1471	410	481158	3997124	1461
90	480841	3997102	1460	420	481169	3997127	1460
100	480851	3997098	1467	430	481177	3997128	1463
110	480861	3997100	1466	440	481188	3997130	1462
120	480871	3997101	1466	450	481196	3997129	1464
130	480880	3997101	1465	460	481207	3997132	1464
140	480889	3997101	1468	470	481217	3997133	1464
150	480899	3997101	1467	480	481228	3997134	1464
160	480911	3997100	1465	490	481239	3997133	1465
170	480921	3997100	1465	500	481247	3997133	1466
180	480930	3997099	1465	510	481256	3997134	1470
190	480941	3997100	1462	520	481266	3997136	1468
200	480950	3997103	1462	530	481276	3997136	1468
210	480956	3997105	1464	540	481286	3997137	1469
220	480968	3997107	1462	550	481296	3997138	1470
230	480980	3997109	1460	560	481306	3997140	1470
240	480989	3997109	1461	570	481316	3997141	1471
250	480997	3997110	1463	580	481326	3997140	1470
260	481009	3997111	1461	590	481336	3997142	1470
270	481018	3997113	1462	600	481345	3997144	1472
280	481026	3997111	1465	610	481356	3997141	1469
290	481038	3997114	1464	620	481365	3997143	1468
300	481048	3997112	1463	630	481375	3997145	1469
310	481057	3997113	1464	640	481385	3997147	1470
320	481067	3997114	1463	650	481396	3997148	1471

**Table 1-4.** Receiver Station Location of each CSAMT electrode for Line D.

[Coordinate system: Universal Transverse Mercator Zone 11, North American Datum of 1983; elevation is in meters above the North American Vertical Datum of 1988]

Electrode identifier	Northing (meters)	Easting (meters)	Elevation (meters)
0	481236	3997547	1466
20	481228	3997527	1466
40	481222	3997509	1465
60	481216	3997489	1466
80	481209	3997471	1467
100	481202	3997453	1468
120	481195	3997433	1467
140	481191	3997412	1466
160	481181	3997396	1464
180	481175	3997378	1465
200	481168	3997358	1460
220	481163	3997339	1463
240	481154	3997321	1464
260	481147	3997302	1461
280	481139	3997281	1465
300	481132	3997262	1468
320	481127	3997244	1468
340	481118	3997228	1465
360	481112	3997207	1466
380	481107	3997188	1465
400	481099	3997168	1467
420	481095	3997154	1461
440	481088	3997135	1461
460	481082	3997117	1467
480	481075	3997098	1462
500	481070	3997078	1462
520	481063	3997058	1462
540	481054	3997042	1462
560	481046	3997024	1461
580	481037	3997006	1460
600	481028	3996988	1461

**Table 1-5.** Receiver Station Location of each CSAMT electrode for Line E.

[Coordinate system: Universal Transverse Mercator Zone 11, North American Datum of 1983; elevation is in meters above the North American Vertical Datum of 1988]

Electrode identifier	Northing (meters)	Easting (meters)	Elevation (meters)
0	481406	3997559	1474
20	481397	3997538	1473
40	481390	3997520	1472
60	481383	3997503	1472
80	481377	3997485	1475
100	481369	3997467	1474
120	481364	3997449	1476
140	481355	3997428	1474
160	481349	3997409	1473
180	481342	3997390	1472
200	481336	3997372	1471
220	481330	3997352	1470
240	481325	3997333	1472
260	481317	3997314	1472
280	481310	3997295	1471
300	481306	3997278	1469
320	481298	3997258	1467
340	481292	3997239	1469
360	481285	3997221	1469
380	481279	3997202	1467
400	481271	3997184	1470
420	481263	3997165	1468
440	481255	3997146	1468
460	481247	3997128	1467
480	481239	3997108	1469
500	481234	3997091	1469
520	481225	3997072	1465
540	481218	3997053	1462
560	481210	3997036	1463
580	481202	3997017	1462
600	481192	3997000	1461

**Table 1-6.** Receiver Station Location of each CSAMT electrode for Line F.

[Coordinate system: Universal Transverse Mercator Zone 11, North American Datum of 1983; elevation is in meters above the North American Vertical Datum of 1988]

Electrode identifier	Northing (meters)	Easting (meters)	Elevation (meters)	Electrode identifier	Northing (meters)	Easting (meters)	Elevation (meters)
0	483263	3991240	1558	660	482604	3991243	1560
20	483241	3991241	1559	680	482584	3991244	1558
40	483221	3991241	1557	700	482563	3991244	1559
60	483203	3991241	1557	720	482544	3991243	1561
80	483183	3991240	1559	740	482524	3991243	1562
100	483164	3991242	1560	760	482504	3991241	1559
120	483145	3991240	1559	780	482485	3991243	1561
140	483124	3991240	1560	800	482464	3991244	1560
160	483103	3991240	1557	820	482444	3991243	1563
180	483084	3991240	1556	840	482423	3991242	1563
200	483065	3991242	1557	860	482405	3991242	1564
220	483043	3991243	1559	880	482384	3991242	1562
240	483024	3991242	1561	900	482364	3991241	1560
260	483005	3991242	1559	920	482345	3991241	1559
280	482984	3991241	1560	940	482325	3991241	1561
300	482964	3991242	1558	960	482304	3991240	1561
320	482943	3991243	1558	980	482286	3991240	1561
340	482923	3991241	1560	1000	482266	3991240	1561
360	482903	3991242	1560	1020	482243	3991241	1559
380	482884	3991242	1558	1040	482224	3991241	1557
400	482864	3991244	1556	1060	482204	3991240	1557
420	482844	3991242	1563	1080	482185	3991240	1557
440	482825	3991243	1562	1100	482164	3991240	1557
460	482805	3991244	1562	1120	482146	3991239	1557
480	482784	3991243	1558	1140	482126	3991238	1558
500	482764	3991243	1559	1160	482106	3991238	1559
520	482744	3991242	1563	1180	482085	3991238	1558
540	482723	3991242	1563	1200	482065	3991239	1558
560	482704	3991242	1562	1220	482044	3991240	1559
580	482684	3991242	1562	1240	482026	3991239	1559
600	482664	3991242	1562	1260	482004	3991239	1557
620	482643	3991242	1559	1280	481984	3991239	1557
640	482622	3991242	1562	1300	481964	3991240	1558

Produced in the Menlo Park Publishing Service Center, California  
Manuscript approved for publication, August 15, 2012  
Text edited by Gail Sladek  
Layout and Design by Jeanne S. DiLeo

